Environmental Science
Processes & Impacts

RSC Publishing

PAPER

Atmospheric particulate matter levels, chemical composition and optical absorbing properties in Camagüey, Cuba

Cite this: *Environ. Sci.: Processes Impacts*, 2013, **15**, 440

Boris Barja,*[a] Sandra Mogo,[bcd] Victoria E. Cachorro,[b] Juan Carlos Antuña,[a] Rene Estevan,[a] Ana Rodrigues[c] and Ángel de Frutos[b]

Atmospheric aerosol particles were collected at Camagüey, Cuba, during the period from February 2008 to April 2009 in order to know the particulate matter levels (PM) together with a general chemical and absorption characterization. The aerosols collection was carried out with a low volume particulate impactor twice a week. Gravimetric analysis of the particulate matter fractions PM10 and PM1 was carried out. An analysis of the eight major inorganic species (Na^+, K^+, Ca^{2+}, Mg^{2+}, NH_4^+, Cl^-, NO_3^- and SO_4^{2-}) using ionic chromatography was conducted. The results were analyzed in two periods, the high aerosol concentration period (May to August) and the period with low aerosol concentration (the other months). During the high concentration period the average PM10 and PM1 levels were 35.11 μg m^{-3} (std = 15.45 μg m^{-3}) and 16.86 μg m^{-3} (std = 6.14 μg m^{-3}). During the low concentration period the average PM10 and PM1 levels were 23.13 μg m^{-3} (std = 5.00 μg m^{-3}) and 13.00 μg m^{-3} (std = 4.02 μg m^{-3}). For both periods, Cl^-, Na^+ and NO_3^- are the predominant species in the coarse fraction (PM1-10), and $SO_4^{2-}$and NH_4^+ are the predominant species in the fine fraction (PM1). The spectral aerosol absorption coefficient, σ_a, was measured for the wavelength range 400–700 nm with 10 nm steps. The σ_a values were obtained with a filter transmission method for the fine fraction and were evaluated for 54 days covering a wide range of atmospheric conditions including a Saharan dust intrusion. σ_a ranges from 8.5 M m^{-1} to 34.5 M m^{-1} at a wavelength of 550 nm, with a mean value of 18.7 M m^{-1}. The absorption Ångström parameter, α_a, calculated for the pair of wavelengths (450/700 nm) presents a mean value of 0.33 (std = 0.19), which is a very low value comparing with those that can be found in the bibliography. Although the sampling period is short, these data represent the first evaluation of PM values with their chemical and optical absorption characterization in Cuba. In addition to the regional interest, the presented values can be directly used by those working with absorption, forcing by aerosols and radiative transfer calculations in general. Also, these data can be used as input in Global Climate Models.

Received 30th July 2012
Accepted 27th November 2012

DOI: 10.1039/c2em30854a

rsc.li/process-impacts

Environmental impact

This work shows the results of the analysis of aerosols and their chemical and optical properties in an understudied area. The Caribbean area is reached by the long range transport aerosols from the Saharan and Sahel regions, and regional transport from the north and south continental regions. Knowledge about the chemical composition and optical characteristics of the aerosols in understudied areas is an issue relevant to the global and international efforts to reduce the natural and anthropogenic impact on the environment. The aerosols or particular matter affect the solar radiation reaching the surface and the terrestrial radiation leaving the earth. They can also affect human health, plants, the ocean and the ecosystems in general.

Introduction

The atmospheric particulate matter (PM) is a mixture of solid, liquid or solid and liquid particles suspended in the air and these mixed states can change the properties of the particles.[1] These particles vary in size, composition and origin and are a significant element in the climate system. It is well known that aerosols affect the climate directly because of their effects on the solar and atmospheric radiation.[2] Aerosols can behave as a

[a]*Grupo de Óptica Atmosférica de Camagüey, Centro Meteorológico de Camagüey, Finlay Av.km 7 ½, Camagüey, 70100, Cuba. E-mail: bbarja@cmw.insmet.cu; Fax: +53 32 262397; Tel: +53 32 262397*
[b]*Grupo de Óptica Atmosférica, Universidad de Valladolid, Spain*
[c]*Universidade da Beira Interior, Portugal*
[d]*Instituto Dom Luis, Portugal*

cooling or warming factor, depending on the process that predominates: the light absorption or scattering. They have also an indirect effect on the climate by modifying physical and radiative properties of clouds. Through this effect they can influence cloud lifetime and precipitation processes. But currently, the knowledge of determining the net effect of aerosols on the climate is still considered to be at a medium-low level of scientific understanding.[3] To evaluate the effects of aerosols on the climate, it is necessary to determine their characteristics. For these reasons atmospheric aerosol studies have increased over the years.

In the visible region of the spectrum the major light-absorbing components present in atmospheric aerosols are black carbon, light absorbing organic carbon (often called "brown carbon") and mineral dust. Soil dust absorbs light in the ultraviolet and visible regions, and some organic components absorb in the ultraviolet region. Strong spectral dependence in the absorption coefficient by organic aerosols in the ultraviolet region has been found in several reported measurements.[4–6] The Ångström absorption exponent (α_a) is used to describe the absorption spectral dependence of light absorbing aerosols. The absorption spectrum of freshly generated diesel soot has an Ångström absorption exponent of 1 with a commonly accepted mass specific absorption coefficient of 10 $m^2\ g^{-1}$ at 550 nm.[7–9] Despite the recent identification of other light absorbing species in the semi-volatile aerosol fraction,[10] it is commonly accepted that black carbon is the main light absorbing aerosol species and it was described by an α_a of 1.[4,7] Bond[11] studied the spectral dependence of visible light absorption by carbonaceous particles emitted from coal combustion and found strong spectral dependency, $1.0 < \alpha_a < 2.9$. A value of $\alpha_a = 1.45$ is reported for biomass burning aerosols in southern Africa.[5] The water soluble polycarboxylic acids known as "humic-like" substances isolated from biomass burning aerosols have very high α_a, in the range of 6 to 7.[12] Fine inorganic dust aerosols have been associated with a wide range of α_a values, from greater than 2 to less than 0.5.[13,14]

As the aerosol properties have a high spatial and temporal variability, it is important to characterize the aerosol properties in different sites of the earth in order to evaluate these properties in a global view. There are numerous reports about the aerosols and PM measurements in the Caribbean. The main results have been reported by the group of Professor Joseph M. Prospero at the University of Miami.[15–20] These studies are related mainly to the arrival to the Caribbean and southeast of the United States of the Saharan dust layer. In Cuba, aerosols' studies started in the 1970s when satellite imaging became available for the first time.[21] There are several studies about the total suspended particles in the atmosphere in some locations of Havana province, near industrial sources.[22] This report shows the values of gaseous pollutants, total suspended particles and their chemical composition. Its results illustrate the contribution of the sea and anthropogenic aerosols. There are also some studies showing the relationship between PM10 levels and the respiratory diseases in Havana city.[23] A measurement campaign of particulate matter (in two particle size fraction PM10 and PM2.5) was carried out in Havana city over five months from November 2006 to April 2007.[24] Authors report the concentrations of 14 elements by the use of the Particle-Induced X-ray Emission (PIXE) technique. Also the origins of the elements were associated with different sources from the region.[24,25] There are no reports in the region about the spectral absorption properties of the aerosols. The scarcity of these types of measurements in the region is the motivation and newness of the present work.

This work reports the analysis of gravimetric measurements of the particulate matter fractions PM10 and PM1 at the Camagüey Meteorological Station site, Cuba. Samples were collected nearly twice a week, during the period from February 2008 to April 2009. The aerosols absorption coefficient (σ_a) measurements are reported and their α_a exponent behavior is analyzed. At the end, a Saharan dust intrusion event is examined.

Methods

Sampling location

The particles were collected in the Meteorological Station of Camagüey, Cuba (21.42° N, 77.85° W, 122 m asl). The station is outside the Camagüey city, at 7 km in the northeast direction, beside the road to Nuevitas city, Fig. 1. The sampling site is located between the road to Nuevitas city and the landing strip of the "Ignacio Agramonte" Airport, in a flat terrain. The distance of the site to both roads is nearly 100 m. The collecting instrument, a particle impactor, is placed in a small cabin built in a terrace, above the roof of the meteorological station. The inlet of the sampling line was approximately 2 m above the roof of the measurement station building, which was approximately 7 m above the ground. There is no high automobile and airplan traffic in the roads. A smaller town is located near the site, 1.0 km in the northeastern direction. Camagüey is a medium size town, with about 325 000 inhabitants, located in the province with the same name in the central-east region of Cuba. There are two seasons that dominate the region, rainy (May to October) and dry (November to April). Climatological variables for the whole province were reported in the Atlas of Camaguey edited by the Cuban Institute of Geography.[26] The mean temperatures in the province are lower in the dry period with 21.1 °C and 22.0 °C for February and January, respectively. In the rainy period the mean temperatures are higher with 27.3 °C and 27.1 °C for July and August, respectively. The annual mean relative humidity in the province is 80%, and increases from 76% in March to 84% in October and November. Diurnal variation of the relative humidity has marked differences with a maximum of 90% at the sunrise time and a minimum of nearly 60% at noontime.[26] The annual precipitation in the province presents a maximum of 1600 mm at the southwest of Camagüey city. This maximum arises almost completely in the rainy period. The number of days with thunderstorms in the province is lower in the dry period, with a mean of 1.59 days. For the rainy period the number of days with electric storm increases sharply, with 88.1 days.[26] The predominant wind direction is from the northeast and east. The location receives also influences of different air

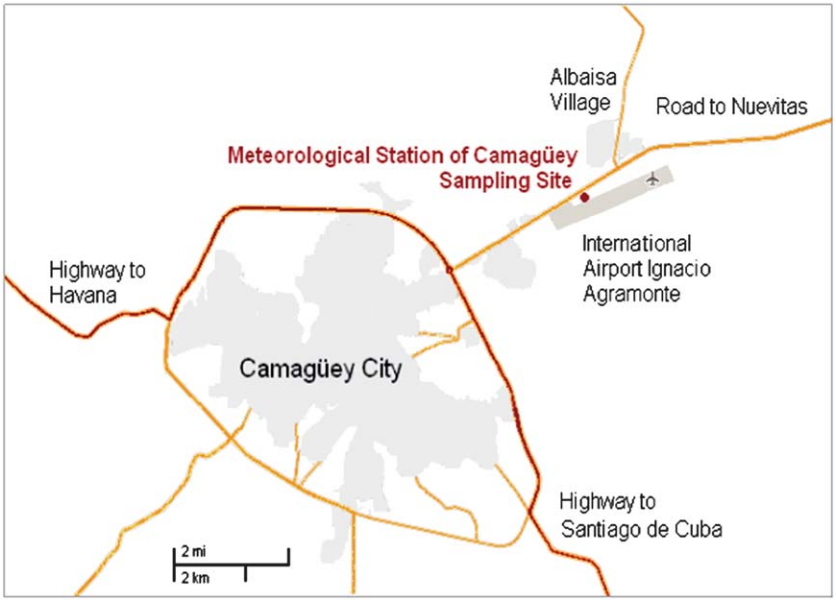

Fig. 1 Map with the location of the measurement site, Meteorological Station of Camagüey (red point), between landing strip of the international airport and road to Nuevitas city. Nearly in the southwest direction is located Camagüey city and Albaisa Village in the northeast direction.

mass origins such as the polar, cold and dry air from the North American continent; tropical, warm and moist air from the Caribbean Sea; and the air from the Atlantic Ocean. The last one has two principal directions, from the northeast, corresponding to trade winds and from the east-southeast. The Saharan desert dust intrusion in Cuba is related to the eastern air mass direction. In July dust events occur in 90% of the days, and between April and August, the frequency of dust events remains above 40%.[21] The Saharan dust is commonly carried in a layer extended from the surface to roughly 3–4 km over the western Atlantic.[27]

Fig. 2(a) shows the monthly mean of the meteorological variables at the site during the measurement period. The data were taken from the tri-hourly meteorological reports from the Camagüey Meteorological Station. Rainfall represents the accumulation of precipitation in the month. Monthly mean of relative humidity has a minimum in April 2009 with 71% and a maximum in December 2008 with 84%. Temperature has a lower mean value in February 2009 with 21.2 °C. The maximum mean value in the temperature was 27.0 °C in July 2008. In the measurement period, precipitations have a minimum of 15.4 mm in January 2009 and a maximum of 430.2 mm in September 2008. The rain from hurricane "Ike" contributes to this maximum. The wind speed has the highest monthly mean value in July 2008 with 15.7 km h^{-1} and the lowest monthly mean value in May 2008 with 9.0 km h^{-1}. The maximum value of wind speed was reached in September 2008, with 80 km h^{-1} from the hurricane "Ike" winds. Calm winds (0 km h^{-1} wind velocity) were more frequent in August 2008, with 26 observations.

Also the wind roses for the rainy and dry seasons in the measurement period are shown in Fig. 2(b). The predominant direction from east is representative of both periods. In the dry period the winds from the northeast increase their frequency.

Sampling method

A Dekati PM10 impactor was used to collect the particles. The particles were deposited over polycarbonate membrane filters with 0.2 μm pores. The flow rate through the impactor was a constant value of 16.5 l min^{-1} during 24 h of measurement. The impactor has three stages with the aerodynamic cutoff diameter of 1 μm and 10 μm. These three stages allow the separation of three PM fractions in the ranges <1 μm (PM1, fine mode), 1 μm to 10 μm (PM1-10, coarse mode) and >10 μm. The impactor is connected to an inlet system and the cut-off diameter of the inlet nozzle and sample transport line was calculated just above 10 μm. Thus, only a residual number of particles actually reach the impactor at the stage above PM10. The filters were weighed before and after collection, in order to obtain the PM mass deposited, based on the gravimetric method. Filters were conditioned in a controlled environment with 20 ± 5 °C temperature and 20 ± 5% relative humidity for a minimum of 24 hours prior to weighing. In order to remove static electricity, the standard procedure of exposing the filters to Polonium 210 was performed.

Experimental methods and dataset

The studied period was from February 2008 to April 2009. The sampling frequency, twice a week, was nearly constant through the whole period, with 97 samples collected. The daily mean concentration of PM was determined as the ratio between the PM mass and the air volume passing through the impactor. There are only 65 sampling days with PM mass concentration out of the whole data due to analytical problems. After October 2008 the balance was out of service.

The analysis was performed by dividing the dataset into two different subsets: the high concentration (HC period) values (May to August) and the low concentration (LC period) values

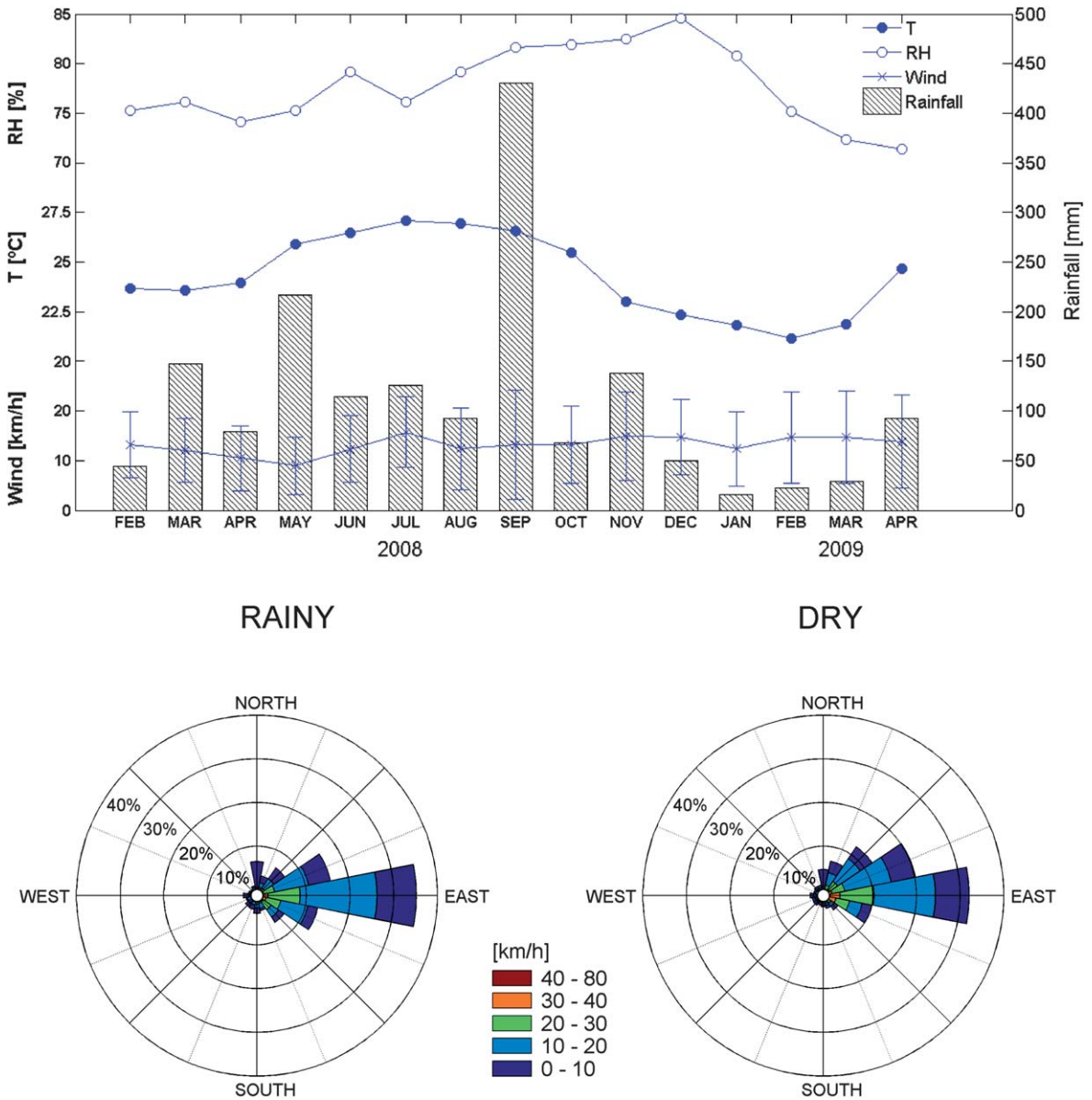

Fig. 2 (a) Monthly mean values of the meteorological variables {Temperature (T), Relative Humidity (RH), Wind Speed (Wind), and Rainfall} in the measurement period (February 2008 to April 2009). The error bars in the wind speed values are standard deviations. (b) Wind roses for the measurement period in the months of the rainy and dry seasons.

(February to April, September and October). These two periods were selected by the arbitrary criteria based on the reports of dusty day frequency in our country.[21] There are 26 sampling days in the HC period and 39 sampling days in the LC period. In the period from August to September 2008, there are only 10 days with measurements, due to three hurricanes that affected the measurement site.

After the gravimetric determination a set of filters was selected for evaluating the concentration of the major ions. This set of filters was formed by 53 filters of PM1-10, and 36 filters of PM1, in the period from February to October 2008. There are 35 days of measurement with information about ions on filters in two stages. The filters were treated with deionized water and the soluble matter was ultrasonically extracted. Samples were placed in an ultrasound bath for an hour and a half. Levels of Cl^-, NO_3^-, SO_4^{2-}, Mg^{2+}, Ca^{2+}, K^+, Na^+ and NH_4^+ were determined by means of ionic chromatography with conductometric detection.[28]

As a first approach to the interpretation of the PM sources, we considered a marine component (obtained from $SO_4^{2-}{}_{(sea\ salt)}$, Cl^- and Na^+), a soil dust component (obtained from K^+/Na^+ and Ca^{2+}/Na^+ ratios) and secondary inorganic phases (obtained from $SO_4^{2-}{}_{(non\text{-}sea\ salt)}$, NH_4^+ and NO_3^-).[34] The amount of SO_4^{2-} in sea salt was calculated as $SO_4^{2-}{}_{(sea\ salt)} = 0.251 \times Na^+$ and the quantity of anthropogenic $SO_4^{2-}{}_{(non\text{-}sea\ salt\ sulfate)}$ was calculated by subtracting the amount of SO_4^{2-} in sea salt from the SO_4^{2-} measured in the atmosphere: $SO_4^{2-}{}_{(non\text{-}sea\ salt\ sulfate)} = SO_4^{2-}{}_{(measured)} - 0.251 \times Na^+$.[35]

A different subset of 50 filters with particle size below 1 μm (PM1) was used to evaluate the spectral aerosol absorption coefficient, in the whole period from February 2008 to April 2009. For the first period from February to October 2008, with 18 selected cases, there is PM mass concentration information. For the second one, from November 2008 to April 2009, with 32 cases, there is no information about the PM mass concentration. Absorption coefficients, σ_a, were evaluated by measurement of light transmission through the exposed filter. The Integrating Sphere Spectral System (IS3) method[29] was used for the determination of σ_a.[30–32] The wavelengths for the σ_a measurements range from 400 nm to 790 nm with 10 nm steps. These methods used to determine the ion concentration and absorption coefficient are destructive, so the filters cannot be used anymore.

The absorption Ångström exponent, α_a, is derived from the absorption spectra for the wavelength pair 450/700 nm using the relationship:

$$\alpha_{a(450/700)} = -\frac{\ln(\sigma_a(700)/\sigma_a(450))}{\ln(700/450)} \quad (1)$$

where $\sigma_a(700)$ and $\sigma_a(450)$ are the absorption coefficients at the wavelengths of 700 nm and 450 nm, respectively. These wavelengths were selected for easier comparison with other authors and instruments, as the case of some nephelometers.

Results and discussions

Seasonal mass concentration and chemical characteristics

Time series of the daily mean mass concentration of PM10 and PM1 are presented in Fig. 3. Data show peaks in PM10 and PM1 concentrations in the period from May to August. These results are in agreement with previous reports in the Caribbean region and the south-eastern region of the United States considering the particularities of the site and the sampling period.[17,33] An important contribution to the PM concentration values in the summer time over the Caribbean is the Saharan dust carried by the synoptic scale transport from the African continent.

The statistical results of PM10 and PM1 concentration data for both periods and all dataset are summarized in Table 1. The average concentration values for LC (HC) periods are 23.13 μg m^{-3} (35.11 μg m^{-3}), 13.00 μg m^{-3} (16.86 μg m^{-3}) and 10.12 μg m^{-3} (18.25 μg m^{-3}) for PM10, PM1 and PM1-10, respectively.

Mean concentration values for PM10, PM1 and PM1-10 are 52%, 30% and 84% higher in the HC period than the respective mean values in the LC period. The standard deviation for PM10 concentration in the HC period is three times the value for LC period. In the case of PM1-10, the standard deviation in the HC period is four times larger than that in the LC period. These characteristics indicate the great dispersion of the data in the HC period compared with the LC period. On the other hand, in the LC period there are small levels of PM10 concentrations.

The differences observed between both periods for PM fractions are statistically significant with 0.05 level of confidence. Although the total particle mass concentrations are significantly different for both periods the fraction of PM1 to

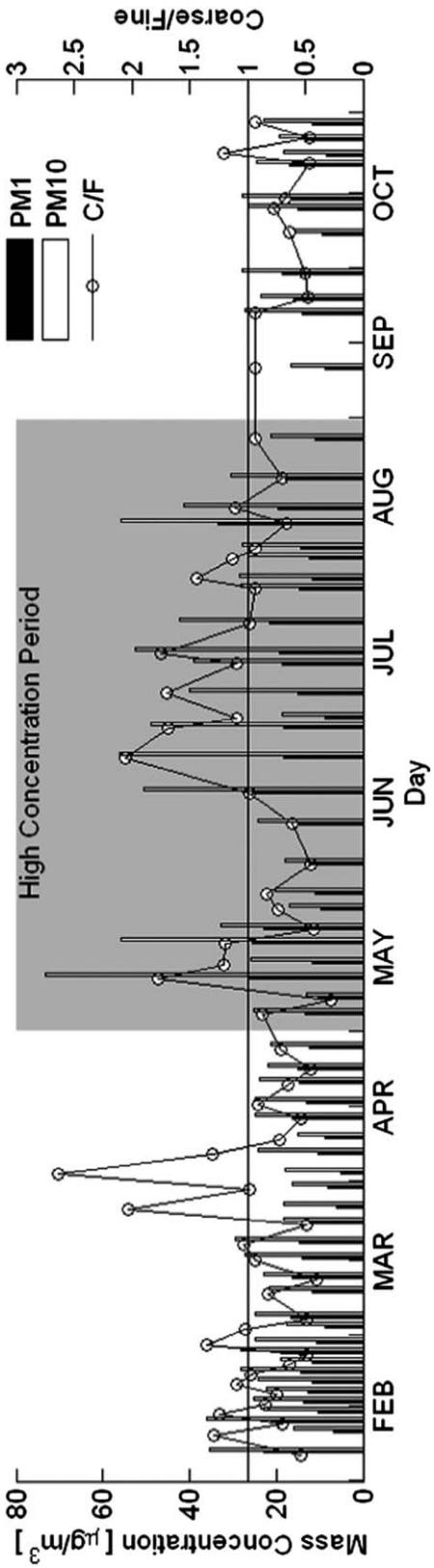

Fig. 3 Daily PM fraction concentration during the measurement period from February 2008 to October 2008. C/F is the ratio between particles with an aerodynamic size above and below 1 μm. The high concentration period (from May to August) is shadowed in the graphic. The low concentration period (February to April, September and October) is not shadowed.

Table 1 Daily mass concentration (μg m^{-3}) statistics for all dataset, low (LC) and high (HC) concentration periods

Period	All			HC			LC		
Fraction	PM10	PM1	PM1-10	PM10	PM1	PM1-10	PM10	PM1	PM1-10
Number of days		65			26			39	
Mean	27.92	14.55	13.37	35.11	16.86	18.25	23.13	13.00	10.12
Max	73.35	33.44	46.94	73.35	33.44	46.94	35.97	22.93	14.92
Min	13.15	4.94	2.85	13.15	8.89	2.85	14.84	4.94	6.04
Std	11.96	5.29	8.13	15.45	6.14	10.81	5.00	4.02	2.63
Quartile 75%	28.71	17.06	13.99	48.93	19.56	24.97	26.16	15.73	12.65
Median	24.91	13.95	11.50	29.40	14.93	14.03	23.45	13.07	9.56
Quartile 25%	20.04	11.04	8.75	24.19	11.68	9.75	18.50	10.32	7.97

PM10 is approximately the same. The ratio between coarse (PM1-10) and fine particles (PM1) (C/F) is also illustrated in Fig. 3. The differences between the LC and HC periods, presented in the statistical analysis, are visually evident in the graphics.

On March 27 and April 3, the ratio C/F presented the highest values registered during the LC period. This strong predominance of the coarse fraction of particles was due to an increase in the concentration of the Na^+ and Cl^- ions and is related to the transport of particles from the Atlantic Ocean to our station. There are two days in the LC period (February 7 and 13, 2008) with values of PM10 concentration greater than 30 μg m^{-3}. These are larger than the mean by more than two standard deviations. The C/F ratios were 0.54 and 0.69 for February 7 and 13, respectively, which indicates the predominance of fine particles. These values are the highest PM1 values registered in the LC period and are produced perhaps due to local particles, because a forest fire took place during these days. This event, observed *in situ*, is further confirmed by the increase in the concentration of K^+ ions which can be used as a marker for wood/vegetative combustion. During the event the K^+ concentration was more than twice that of the mean.

In the case of HC period, May 12, 2008 had the maximum PM10 concentration value of 73.3 μg m^{-3}, which is at least two standard deviations larger than the mean. The conditions for this day were analyzed and showed high levels of pollution, related to high NO_3^- and SO_4^{2-} ions concentration, mixed with possible marine aerosols and/or dust, related to reasonably high concentrations of Ca^{2+}, K^+, Na^+ and Cl^-. The direction of the wind was from the southwest throughout almost all of the measurement time. From reanalysis data the air mass measured seems to be a mixture of the Saharan dust clouds, marine aerosols and perhaps pollution aerosols from the northern region of the South American continent.

Some peaks in Fig. 3 are related to the incidence of Saharan dust intrusions in our region. An example is the June 25, 2008, with an evident presence of the aerosol cloud from the Saharan dust over the Caribbean. Also in this case, the measured air mass seems to be a mixture of the Saharan dust clouds, marine aerosols and perhaps pollution aerosols from the local and regional sources.

Regarding ion chemical composition, Table 2 shows the ion concentration for both periods and the average values registered during Saharan dust events. The ionic content of PM is a significant fraction of the total PM mass, with ~45% in both the fine and the coarse fractions. The mean ion balance in PM10, expressed by the ratio of anion to cation concentrations (Σ^-/Σ^+), is 1.4. The dominant components in the descending order for the fine fraction are SO_4^{2-}, NH_4^+, Ca^{2+} and K^+, whereas those for the coarse fraction are Cl^-, Na^+, NO_3^- and SO_4^{2-}. For the fine fraction, Na^+, NH_4^+, K^+, Ca^{2+}, Cl^- and NO_3^- are higher in the LC period, while SO_4^{2-} is higher in the HC period. For the coarse

Table 2 Concentration (μg m^{-3}) for major ionic components measured at Camagüey for the two periods studied and for the sampling Saharan dust events. The anthropogenic SO_4^{2-} obtained by calculation and their fraction R_{as} in the total particle mass are also shown

	All		HC		LC		Saharan dust events	
Period	PM1 (fine)	PM1-10 (coarse)	PM1 (fine)	PM1-10 (coarse)	PM1 (fine)	PM1-10 (coarse)	PM1 (fine)	PM1-10 (coarse)
PM	14.55	13.37	16.86	18.25	13.00	10.12	16.77	21.69
Na^+	0.29	1.58	0.22	1.57	0.38	1.59	0.25	1.75
NH_4^+	1.87	0.01	1.61	0.01	2.18	0.01	1.3	0.02
K^+	0.63	0.17	0.38	0.19	0.92	0.15	0.41	0.22
Mg^{2+}	0.03	0.20	0.04	0.21	0.02	0.19	0.05	0.27
Ca^{2+}	0.68	0.30	0.44	0.43	0.96	0.18	0.40	0.58
Cl^-	0.33	2.36	0.29	2.50	0.37	2.24	0.27	3.33
NO_3^-	0.44	1.06	0.38	1.15	0.51	0.99	0.40	1.30
SO_4^{2-}	2.45	0.73	2.55	0.92	2.34	0.58	2.63	1.03
SO_4^{2-} (non-sea salt sulfate)	2.30	0.34	2.49	0.53	2.25	0.18	2.56	0.53
R_{as} (%)	16.40	2.50	14.80	2.90	17.30	1.80	15.30	2.40

fraction, Ca^{2+}, Cl^-, NO_3^- and SO_4^{2-} are higher in the HC period, while Na^+, NH_4^+, K^+, and Mg^{2+} are approximately the same. There are statistically significant differences in the concentration of Na^+, K^+, Ca^{2+} ions between both periods for the fine mode with 0.05 confidence level. Note that in the fine mode concentrations of the SO_4^{2-} and NH_4^+ in both periods have the largest values. Sulfates and ammonium have a great contribution in the fine mode. On the other hand, the major coarse mode species are Cl^-, Na^+ and NO_3^- ions from the sea salts in both seasons.

The anthropogenic sulfate is slightly higher in the HC period, but the fraction of anthropogenic sulfate in the total particles (R_{as}) is higher in the fine mode for the LC period. The joint contributions from the coarse and fine particles denoted by the fraction of the anthropogenic sulfate in both periods are similar. The mean ionic ratio of Cl^-/Na^+ is 1.3 and comparing with the values expected for seawater (1.16) and earth's crust (0.003), our value is closer to the value expected for seawater, denoting the contribution of sea salt to the ambient concentration of Cl^-.[36–38] The K^+/Na^+ mean ratio is 0.4, nearly the value expected for soils (0.45),[36] indicating that the presence of potassium can be mainly attributed to soil dust. Finally, the contribution of the secondary inorganic phases to the PM10 presented an average value of 26%, ranging from 10% to 56%.

Absorption coefficient and absorption Ångström exponent

Fig. 4 shows the temporal evolution of the absorption coefficient, σ_a, at a wavelength of 550 nm. Note that from July to October, there is a gap in the absorption measurements. More filters were selected for evaluating the concentration of ions by ionic chromatography in this month, because of the greater frequency of Saharan desert dust intrusions. As the methods used to determine the ion concentration and absorption coefficient are both destructive, the filter can be used only to determine one magnitude.

From February to October 2008, almost all selected days have background conditions, with low concentration levels of PM. From November 2008 to April 2009, there is no information about the PM levels, because the balance was out of service. The absorption coefficients at 550 nm are in the range of 8.5 M m^{-1} to 34.5 M m^{-1}, with a mean of 18.7 M m^{-1}. As long as we know, there are no other σ_a values reported for the Caribbean region, so we compare our values with other data measured by the Atmospheric Optics Group of the University of Valladolid (GOA-UVa) using the same techniques presented in this work. The values obtained in Camagüey are lower than those reported in Europe for urban environments but higher than those reported for rural and remote places. Daily values from 7.0 M m^{-1} to 100.0 M m^{-1} at a wavelength of 550 nm were reported in Valladolid, Spain,[39] a medium size town with ~500 000 inhabitants located in the north-center of the Iberian Peninsula. Also, for a non-urban station in south Spain, El Arenosillo, located in the neighborhood of a nature-protected area, the values of σ_a at 550 nm range from 0.09 M m^{-1} to 2.31 M m^{-1}, with an average value of 0.88 M m^{-1}.[36] Daily means are reported for Andenes, Norway with values from 0.02 M m^{-1} to 1.50 M m^{-1} at 520 nm.[29]

The absorption Ångström exponent, α_a, characterizes the spectral features of the absorption coefficient. In our case, it is calculated for the pair of wavelengths 450/700 nm, as previously mentioned. The temporal behavior of α_a is shown also in Fig. 4. α_a values range from 0.01 to 1.0 with a mean value of 0.3 (std = 0.2).

There are three days with a distinct spectral behavior in the absorption coefficient, corresponding to the extreme values of α_a. The absorption coefficients for February 17, 2008 and April 13, 2009 have a sharp decrease with the increase of the wavelengths, with value of α_a reaching 1.0. The absorption coefficient decreases the magnitude by 64% between the wavelengths of 450 nm and 700 nm. The $\alpha_a = 1$, values for these days match with the values reported in the literature representative of the black carbon.[4,7] The smallest value of α_a (0.01) that is the smallest variation of the absorption coefficient with wavelength was found on August 11, 2008. This means that the absorption coefficient is almost constant; its magnitude at 700 nm is 99.6% of the value at 450 nm. This day shows the maximum absorption coefficient in all measured days.

As we have spectral information of the absorption coefficient from 400 to 790 nm, we show in Table 3 the mean, minimum and maximum (standard deviation in parentheses) of absorption coefficients for several wavelengths covering the above referred spectral range. For our limit of wavelengths, 400 nm and 790 nm, the average absorption coefficients measured are 20.3 M m^{-1} and 16.8 M m^{-1}, respectively.

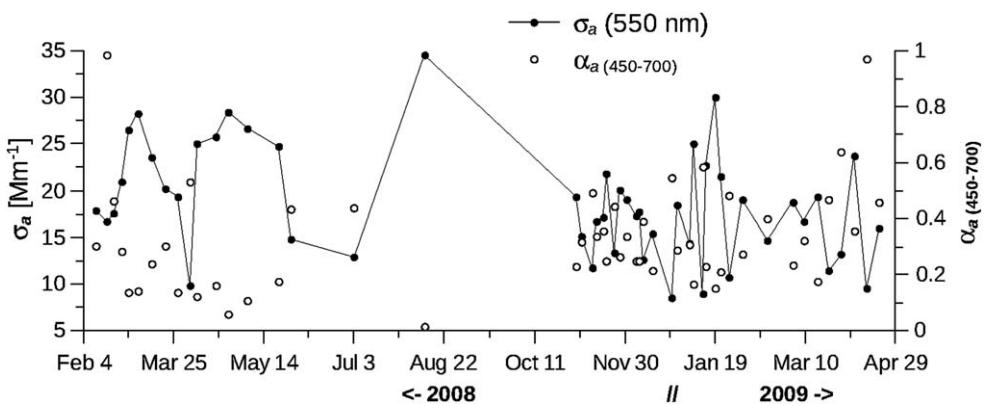

Fig. 4 Time-series of daily values of absorption coefficient at a wavelength of 550 nm and absorption Ångström exponent for the pair of wavelengths 450/700 nm.

Table 3 Evaluation of the overall ranges and arithmetic mean of the daily values of σ_a and α_a. The wavelengths presented were selected throughout our spectral data according to the wavelengths used by other instrumentation (Cimel, TOMS) in order to facilitate comparison of data

	σ_a (M m^{-1})						
Wavelength (nm)	Mean	Std	Max	Min	Median	Quartile 25%	Quartile 75%
400	20.3	5.7	35.1	9.6	20.0	15.9	23.9
450	19.7	5.8	34.8	9.3	19.5	15.6	23.4
550	18.7	5.9	34.5	8.5	18.2	14.7	22.5
670	17.6	6.1	34.5	7.5	17.0	13.6	21.4
700	17.4	6.2	34.6	7.3	16.7	13.3	21.2
790	16.8	6.3	35.1	6.5	15.8	12.6	20.3
α_a (450/700 nm)	0.3	0.2	1.0	0.01	0.3	0.2	0.4

The α_a exponents as a function of σ_a at 550 nm are presented in Fig. 5. There is a notable negative linear relationship between these two variables. Days with the lowest values for α_a have also the highest values of σ_a. Days with the highest values of α_a, on the other hand, have the lowest σ_a. So the aerosols with high/low absorption measured in this site show low/high spectral variation. This behavior suggests the presence of two types of aerosols. Due to the limited number of measurement days, it is impossible to make an extensive analysis of this aspect.

Freshly emitted black carbon particles have been reported to present α_a around 1.[7,9,40] As also reported by Lack and Cappa[41] the α_a values for black carbon cores can vary around 1 but within a large range, from −0.2 to 1.3, depending on the size of the particles. Other studies show that the α_a for organic species is larger than for black carbon.[10] Fine dust aerosols have been related to a large range of α_a values, from as low as 0.5 to as high as 3.2.[14,42] In Valladolid, the GOA-UVa registered values in the range of 0.1 to 2.5 (400–650 nm),[39] and in the station of El Arenosillo, the values ranged between 0.2 and 2.0 (400–800 nm).[32] Both locations were frequently affected by Saharan dust intrusions. On the other hand, the nearest ground data we could find from the Camagüey station were obtained by Marley *et al.*[43] from aethalometer absorption measurements made in Mexico city in April 2003 and March 2006. The authors found a range of α_a from 0.63 to 1.5, calculated from the absorption measurements at seven wavelengths from 370 nm to 950 nm.

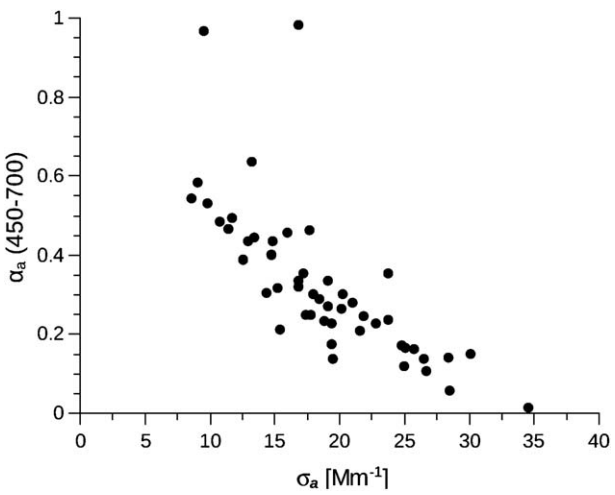

Fig. 5 Daily values of the absorption coefficient at 550 nm as a function of the absorption Ångström exponent for the pair of wavelengths 450/700 nm.

Because no other data are available for this region, we have no possibility to compare our results with other authors or with near and similar regions. However, the columnar data of spectral absorption optical depth have been presented for several field programs, for example by Bergstrom *et al.*[13] and Russell *et al.*[5] They show spectral absorption properties of aerosols for different regions from the field programs SAFARI 2000 (Southern African Regional Science Iniciative), PRIDE 2000 (Puerto Rico Dust Experiment), ACE Asia 2001 (Aerosol Characterization Experiment) and experiments with North Atlantic urban aerosols in the coast of United States, TARFOX 1996 and ICARTT 2004 (Tropospheric Aerosol Radiative Forcing Observational Experiment and International Consortium for Atmospheric Research on Transport and Transformation). In these studies, the spectral absorption optical depth is described as decreasing with the wavelength and can be approximated with the power-law wavelength dependence. This is also shown in Bergstrom *et al.*[44] with measurements from MILAGRO/INTEX-B 2006 (Megacity Initiative-Local And Global Research Observations/Phase B of the Intercontinental Chemical Transport Experiment) field campaign. Bergstrom *et al.*[13] show some measurements of α_a with values lower than 1 for Houston during GoMACCS (Gulf of Mexico Atmospheric Composition and Climate Study, August–September, 2006) field campaign. The GoMACCS measurements of α_a are from shipborne measurements ranging from 0.3 to 3 with mean values of 0.84, 0.91 and 1.07 for wavelength pairs 530/660 nm, 467/660 nm, and 467/530 nm, respectively.[5] However, the correlation between columnar values and surface *in situ* values can only indicate how representative the surface measurements are of the atmospheric column and direct relationship in all situations is not expected.

Despite the differences between the present study and the aforementioned reports regarding wavelength intervals and instruments used in the measurements, our mean value of α_a is located in the lower range of the values reported in these studies. The optical characteristics of the aerosols in Camagüey during the studied period are associated with a mixed aerosol type. The results show the presence of aerosols in the atmosphere of Camagüey site with low absorption coefficients and absorption Ångström exponents. These features based on the chemical analyses indicate the presence of high concentration of scattering components such as sulfate and ammonium components.

Saharan dust intrusions

The contribution of long range transported particles to the PM and ionic concentrations during several dust events was also estimated. A total of four dust events were sampled over the entire study period. The mean concentrations of fine and coarse

particles when the air masses passed over Cuba were 16.77 μg m^{-3} and 21.69 μg m^{-3}, respectively. As a result, the average concentrations of fine and coarse particles measured under dust conditions were 15% and 62% higher than their mean values obtained for the complete measurement period, as shown in Table 2. Our observations show that during the dust events, concentrations increased for all ionic species. Under these circumstances, Ca^{2+} and non-sea salt sulfate become important contributors to the coarse mode. The longest dust event during the study period occurred in mid-July 2008 and lasted for several days, with a PM10 peak concentration of 52.52 μg m^{-3}. The strongest dust event occurred in May 2008 and had a PM10 peak concentration of 73 μg m^{-3}. The mean value of PM10 mass concentration for all the desert event samplings during the measurement period is 59.39 μg m^{-3}. The event of August 2008 provides an example of a typical case of Saharan dust transport affecting Cuba and it will be discussed to illustrate the results of this study.

During the first few days of August 2008, an intense Saharan dust cloud left the African continent in the direction of the Caribbean Sea Region. This aerosol clouds reached the Camagüey site on August 8th. Three samples of the air were taken from our location around cloud arrival day on August 6, 11, and 14, before, during and after the intrusion, respectively. Only August 11 has absorption coefficient measurements, but there is no chemical ion determination as both techniques are destructive. Both days, August 6 and 14, have chemical characterizations.

As we can see in Fig. 3, August 11 presents the highest values of mass concentration for these three days, with a PM10, PM1 and PM1-10 of 55.73 μg m^{-3}, 33.44 μg m^{-3} and 22.28 μg m^{-3}, respectively (Table 4). There is higher concentration of fine than coarse particles with a C/F ratio of 0.67. This result is different from the Saharan dust intrusion registered on June 25, 2008, where the coarse fraction is higher than the fine fraction, with a C/F ratio of 2.1 (June 25 presents the highest value of the C/F ratio in the HC period).

In the present case of study, August 11 is the fourth day under the cloud influence. So we can hypothesize that the fine particles remain in the atmosphere and coarse ones precipitate. Table 4 shows a quick increase in the particle concentration from August 6 to August 11, to nearly twice that in PM10. Also, a slow decrease is shown from August 11 to August 14, in all fractions of particle concentrations, denoting the end of the event. This decrease is maintained up to September 11, Fig. 3.

Table 5 shows the concentrations of ion components for three days analyzed with the Saharan dust intrusion, in the fine and coarse mode. As we said previously, it was not possible to analyze the ionic behavior in the fine mode because there was no chemical ion concentration information for PM1 on August 11. On the other side, for the coarse mode, the concentrations of Ca^{2+} and NO_3^- increase, while all the other ions decrease. These aspects show the influence of the dust aerosols with particles of calcium and the presence of high levels of NO_3^- probably due to the absorption of HNO_3 gas by the coarse particles carrying Ca^{2+} ions, which have a basic character.[45]

Fig. 6(a) shows the local wind roses during the 24 h measurement interval for each sample day. On the first day a northeast direction of the wind was more frequent with 81%, while on the second day the southwest direction was more frequent with 31%. On the last day the frequent wind direction was towards the east with 54%. These three directions are related to the high concentration of PM. Fig. 6(b–d) show the backward trajectories for each day of study. The backward trajectories were calculated with a duration of 5 days starting at 14 UTC. The graphics show that the air mass origin was in the eastern Atlantic for the first and second days. For the last day the origin was in the southeastern Atlantic. For August 11, the day with maximum PM10 concentration, the air mass moved through the Caribbean Sea and the southern region of the site, thus it should be composed of a mixture of Saharan dust clouds and marine aerosols.

To further analyze this event, we present the aerosol index (AI), a product from the Ozone Monitoring Instrument (OMI) that is a measure of how back-scattered ultraviolet radiation from an atmosphere containing aerosols differs from that of a pure molecular atmosphere. The AI is very sensitive to the presence of UV absorbing aerosols such as smoke or mineral dust and it is expected to be positive when absorbing aerosols are present.

The AIs for each day in the interval of measurements are shown in Fig. 7. The AIs in the first few days of August (not shown) confirm high values of AI in the western of the African continent. It seems to have a low concentration of aerosols in the Caribbean. During the five to six following days the Saharan dust is transported through the Atlantic. The upper panel in Fig. 7 shows the AI for August 6 and August 7. The area at the east of Cuba is affected by the clouds of Saharan dust aerosols with moderate intensity. Table 4 shows the PM10 concentration for August 6, with a value of 27.94 μg m^{-3}, similar to the mean concentration for all datasets, 27.92 μg m^{-3}. August 11 shows lower values of AI than August 6 (middle panel). But the value of PM10 concentration is 55.76 μg m^{-3} (Table 4), which is higher than the mean value for the HC period. This means that our filter did not pick up the peak of the event, collecting just in the beginning of the event arrival (filter from August 6) and just after the maximum peak of the event (filter from August 11). We assume that there are present remains of the dust cloud, seen in the upper panel for August 6. In the lower panel of Fig. 7, the AI denotes the presence of aerosols in the area, but with low values of the AI.

The spectral behavior of the absorption coefficient for the day August 11, expressed by the absorption Ångström exponent can be seen in Fig. 4. A slow decrease of the absorption coefficient with the wavelength is shown by the minimum value of α_a.

Table 4 Daily mass concentration for three days of the Saharan dust intrusion period on August 6, 11, and 14

	PM10 (μg m^{-3})	PM1 (μg m^{-3})	PM1-10 (μg m^{-3})
August 6	27.94	14.47	13.46
August 11	55.73	33.44	22.28
August 14	41.26	19.56	21.70

Table 5 Concentration (μg m^{-3}) for major ionic components measured at Camagüey for three days of the Saharan dust intrusion period on August 6, 11, and 14

	August 6		August 11		August 14	
	PM1 (μg m^{-3})	PM1-10 (μg m^{-3})	PM1 (μg m^{-3})	PM1-10 (μg m^{-3})	PM1 (μg m^{-3})	PM1-10 (μg m^{-3})
Na^+	0.18	1.31	—	0.56	0.19	1.05
NH_4^+	1.95	0	—	0.002	1.56	0
K^+	0.35	0.23	—	0.21	0.28	0.15
Mg^{2+}	0.06	0.15	—	0.09	0.08	0.14
Ca^{2+}	0.37	0.30	—	0.63	0.39	0.56
Cl^-	0.20	1.99	—	0.68	0.15	1.59
NO_3^-	0	0.77	—	1.21	0.33	0.93
SO_4^{2-}	2.25	0.66	—	0.46	2.04	0.70

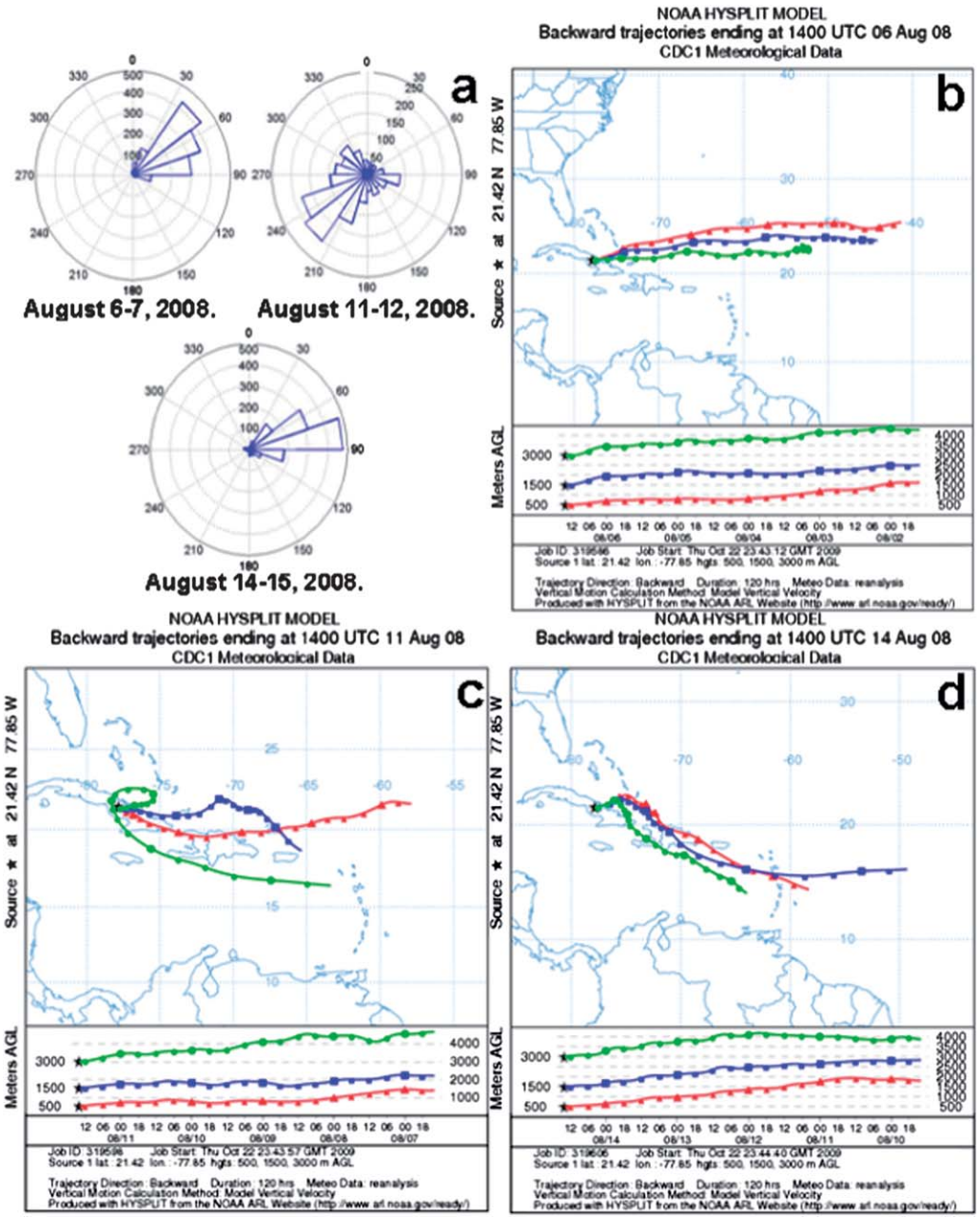

Fig. 6 (a) Wind roses during the measurement interval (24 hours) for each day of samples. (b–d) Backward trajectories calculated from HYSPLIT model at 14:00 UTC on August 6, 11 and 14, 2008.

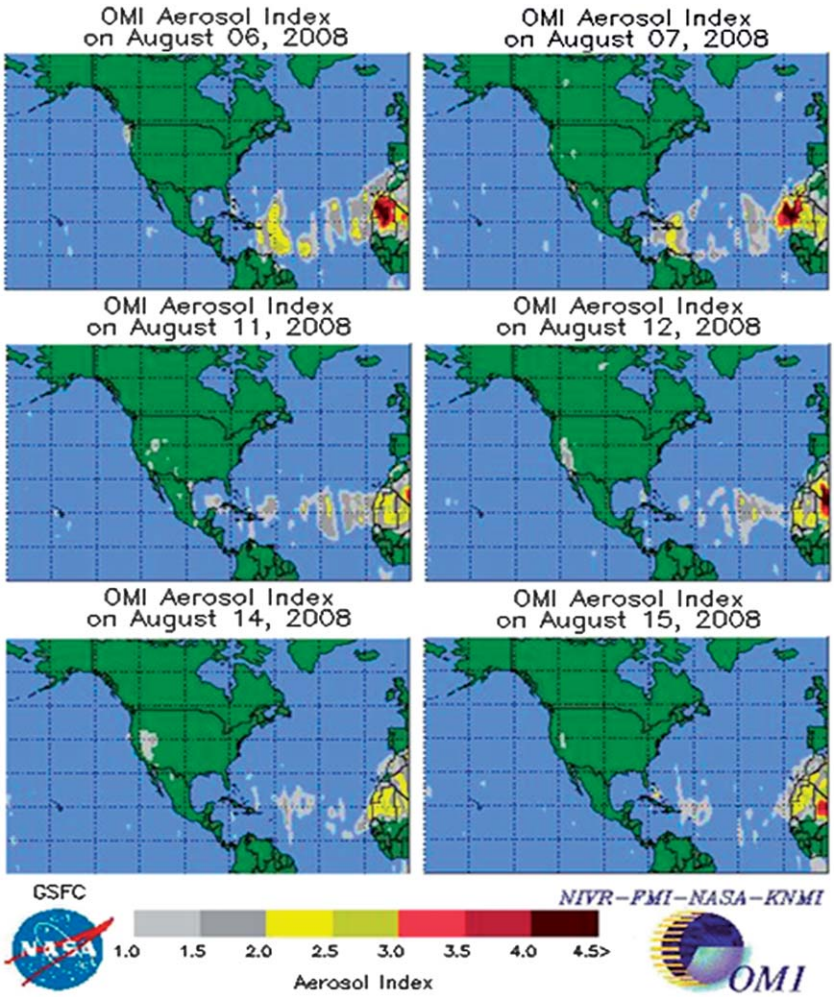

Fig. 7 Aerosol Index from Ozone Monitoring Instrument (OMI) for each pair of measurement days.

The value of the absorption Ångström coefficient between wavelengths of 450 nm and 700 nm for this day is 0.01. This small value, the lowest registered, expresses the almost flat shape of the absorption coefficient spectrum. This value suggests the presence of fine dust particles, consequent with the conditions in the area, the presence of the Saharan dust cloud remains.

Summary and conclusions

The newness of the present report is based on the scarcity of the measurements of the particle's concentration and the spectral absorption properties of the aerosols in the region. As long as the authors know there are no previous reports from medium sized towns or even for rural areas over Cuba. The technical difficulties associated with the local measurements, including problems with the maintenance of the instrumentation, are an explanation for this scarcity. To the technical problems, one must also add the problems associated with the existing infrastructure and logistic questions.

Characterization of the PM10 and PM1 fraction concentrations and their chemical composition at Camagüey, Cuba are reported for the period from February to October 2008. The mean values of PM10 and PM1 are 27.92 μg m^{-3} and 14.55 μg m^{-3}, respectively. The highest concentration of PM is observed between May and August. An analysis in two periods is carried out, period with low concentration (LC) and period with high concentration (HC) of aerosols. Means of PM10 are 23.13 μg m^{-3} and 35.11 μg m^{-3}, for the LC and HC periods, respectively. There are differences between both periods for PM fractions statistically significant with 0.05 level of confidence. There are also statistically significant differences in the concentration of Na^+, K^+, Ca^{2+} ions between both periods for the fine mode, with 0.05 confidence level. Note that in the fine mode, concentrations of SO_4^{2-} and NH_4^+ in both periods have the largest values. Sulfates and ammonium have a strong contribution for the fine mode. On the other hand, for the coarse mode the main contributions are from Na^+, Cl^- and NO_3^- ions. During dust events, Ca^{2+} and non-sea-salt sulfate also increase their contribution to the coarse mode significantly. The observation of C/F values above the mean is due to the increase in the concentrations of Na^+ and Cl^- ions and is related to the transport of particles from the Atlantic Ocean to our station. These situations may or may not coincide with a dust event.

The spectral aerosol absorption coefficient for PM1 was evaluated until April 2009. The absorption coefficient values range from 8.5 M m^{-1} to 34.5 M m^{-1} at a wavelength of 550 nm, with a mean value of 18.7 M m^{-1}. The absorption Ångström exponents between wavelengths of 450 nm and 700 nm are calculated and the mean value of α_a is 0.33 with a standard deviation of 0.19. The aerosols have variable spectral behavior of the absorption, presenting high/low α_a for the lowest/highest absorbing particles.

The present study is the first to characterize the dust events occurring in Camagüey, Cuba. The study shows the scale and importance of dust events in the region and the characteristics of these events. The concentration of PM10 during the dust events increases by 113%. A total of four dust events and 13 dusty days occurred in the study area over the entire study period. These occurrences took place in the period from May to August. The longest dust event during the study period occurred in July. It lasted for several days and had a PM10 peak concentration of 52.52 μg m^{-3}. The event associated with the highest level of PM10 had a peak concentration of 73 μg m^{-3}. The occurrence of prevailing eastern air masses during dust events supported the hypothesis that Sahara is the source of the events in our area.

Acknowledgements

Authors thank the staff of the Air Quality Lab at the National Institute for Hygiene and Epidemiology and Microbiology in Havana City (INHEM) for their fundamental contribution in weighing the filters. Authors from GOAC-INSMET want to thank the GOA-UVa team for the support and logistic. We would also like to thank the NOAA Air Resources Laboratory for providing the HYSPLIT[46] model use online. Finally, the authors wish to thank those who sought to improve the quality of this paper with their comments and suggestions and are particularly grateful to the reviewers. This work has been supported by the Cuban National Climate Change Research Program and by the Collaboration Agreement between the Grupo de Óptica Atmosférica (GOA-UVA) and the Grupo de Óptica Atmosférica de Camagüey (GOAC-INSMET), formerly the Camagüey Lidar Station and Financial supports from the Spanish MICIIN (ref. CGL2008-05939-CO3-00/CLI and CGL 2009-09740).

References

1 S. Chandra, S. Satheest and J. Srinivasan, Can the state of mixing of black carbon aerosols explain the mystery of 'excess' atmospheric absorption?, *Geophys. Res. Lett.*, 2004, **31**, L19109.

2 J. Haywood and O. Boucher, Estimates of the Direct and Indirect Radiative Forcing Due to Tropospheric Aerosols: A Review, *Rev. Geophys.*, 2002, **38**(4), 513–543.

3 IPCC, *Climate Change. The Physical Science Basis. Contribution of Working Group I to the Fourth Assessment Report of the Intergovernmental Panel on Climate Change*, ed. S. Solomon, D. Qin, M. Manning, Z. Chen, M. Marquis, K. B. Averyt, M. Tignor and H. L. Miller, Cambridge University Press, Cambridge, United Kingdom and New York, NY, USA, 2007, p. 996.

4 T. W. Kirchstetter, T. Novakov and P. V. Hobbs, Evidence that the spectral dependence of light absorption by aerosols is affected by organic carbon, *J. Geophys. Res.*, 2004, **109**, D21208, DOI: 10.1029/2004JD004999.

5 P. B. Russell, R. W. Bergstrom, Y. Shinozuka, A. D. Clarke, P. F. De-Carlo, J. L. Jimenez, J. M. Livingston, J. Redemann, O. Dubovik and A. Strawa, Absorption Angstrom Exponent in AERONET and related data as an indicator of aerosol composition, *Atmos. Chem. Phys.*, 2010, **10**, 1155–1169, DOI: 10.5194/acp-10-1155-2010.

6 M. Yang, S. G. Howell, J. Zhuang and B. J. Huebert, Attribution of aerosol light absorption to black carbon, brown carbon, and dust in China - interpretations of atmospheric measurements during EAST-AIRE, *Atmos. Chem. Phys.*, 2009, **9**, 2035–2050, DOI: 10.5194/acp-9-2035-2009.

7 R. W. Bergstrom, P. B. Russell and P. Hignett, The wavelength dependence of the absorption of black carbon particles: predictions and results from the TARFOX experiment and implications for the aerosol single scattering albedo, *J. Atmos. Sci.*, 2002, **59**, 567–577.

8 C. F. Bohren and D. R. Huffman, *Absorption and scattering of light by small particles*, John Wiley & Sons, New York, 1983.

9 N. A. Marley, J. S. Gaffney, J. C. Baird, C. A. Blazer, P. J. Drayton and J. E. Frederick, The determination of scattering and absorption coefficients of size-fractionated aerosols for radiative transfer calculations, *Aerosol Sci. Technol.*, 2001, **34**, 535–549.

10 M. O. Andreae and A. Gelencsér, Black carbon or brown carbon? The nature of light-absorbing carbonaceous aerosols, *Atmos. Chem. Phys.*, 2006, **6**, 3131–3148.

11 T. C. Bond, Spectral dependence of visible light absorption by carbonaceous particles emitted from coal combustion, *Geophys. Res. Lett.*, 2001, **28**(21), 4075–4078, DOI: 10.1029/2001GL013652.

12 A. Hoffer, A. Gelencsér, P. Guyon, G. Kiss, O. Schmid, G. P. Frank, P. Artaxo and M. O. Andreae, Optical properties of humic-like substances (HULIS) in biomass-burning aerosols, *Atmos. Chem. Phys.*, 2006, **6**, 3563–3570, DOI: 10.5194/acp-6-3563-2006.

13 R. W. Bergstrom, P. Pilewskie, P. B. Russell, J. Redemann, T. C. Bond, P. K. Quinn and B. Sierau, Spectral absorption properties of atmospheric aerosols, *Atmos. Chem. Phys.*, 2007, **7**, 5937–5943.

14 D. Meloni, A. di Sarra, G. Pace and F. Monteleone, Aerosol optical properties at Lampedusa (Central Mediterranean). 2. Determination of single scattering albedo at two wavelengths for different aerosol types, *Atmos. Chem. Phys.*, 2006, **6**, 715–727.

15 I. Chiapello, C. Moulin and J. M. Prospero, Understanding the long-term variability of African dust transport across the Atlantic as recorded in both Barbados surface concentrations and large-scale Total Ozone Mapping Spectrometer (TOMS) optical thickness, *J. Geophys. Res.*, 2005, **110**, D18S10, DOI: 10.1029/2004JD005132.

16 J. M. Prospero, E. Bonatti, C. Schubert and T. N. Carlson, Dust in the Caribbean atmosphere traced to an African dust storm, *Earth Planet. Sci. Lett.*, 1970, **9**, 287–293.
17 J. M. Prospero, Long-term measurements of the transport of African mineral dust to the southeastern United States: Implications for regional air quality, *J. Geophys. Res.*, 1999, **104**(D13), 15917–15927.
18 J. M. Prospero, I. Olmez and M. Ames, Al and Fe in PM 2.5 and PM 10 suspended particles in South-Central Florida: The impact of the long range transport of African mineral dust, *Water, Air, Soil Pollut.*, 2001, **125**, 291–317.
19 J. M. Prospero, W. M. Landing and M. Schulz, African dust deposition to Florida: Temporal and spatialvariability and comparisons to models, *J. Geophys. Res.*, 2010, **115**, D13304, DOI: 10.1029/2009JD012773.
20 J. M. Trapp, F. J. Millero and J. M. Prospero, Temporal variability of the elemental composition of African dust measured in trade wind aerosols at Barbados and Miami, *Mar. Chem.*, 2008, DOI: 10.1016/j.marchem.2008.10.004.
21 E. Mojena, P. Ortíz, A. Ortega and A. Rivero, Tormentas de Polvo del Sahara. Su impacto en el Atlántico, Mar Caribe y el Golfo de México, *Revista Cubana de Meteorología*, 2006, **13**(1), 99–100.
22 O. Cuesta, A. Wallo, A. Collazo, P. Sánchez, M. González and R. Labrador, Aspectos de la composición química del aire en la zona de la ribera este de la Bahía de La Habana, *Revista Cubana de Meteorología*, 2002, **9**(2), 90–99.
23 E. Molina, L. A. Brown, V. Prieto, M. Bonet and L. Cuéllar, Crisis de asma y enfermedades respiratorias agudas, contaminantes atmosféricos y variables meteorológicas en Centro Habana, *Rev. Cubana Med. Gen. Integr.*, 2001, **17**(1), 10–20.
24 G. Pérez, I. Piñera, M. Ramos, R. Guibert, E. Molina, M. Martínez, A. Fernández, F. Aldape and J. Flores, *PIXE analysis and source identification of airborne particulate matter collected in downtown Havana City. VI international symposium on nuclear & related techniques. XII workshop on nuclear physics*, Instituto Superior de Tecnologías y Ciencias Aplicadas (InSTEC), Havana, Cuba, 9–12 February, 2009, ISBN 978-959-7136-62-0.
25 I. Piñera, G. Pérez, F. Aldape, J. Flores, E. Molina, M. Ramos, M. Martínez and R. Guibert, *Estudio de Partículas Finas de la Atmósfera en Centro Habana. Contrib. Educ. Prot. Med. Amb.*, (In Spanish) Instituto Superior de Tecnologías y Ciencias Aplicadas (InSTEC), Cuba, 2010, vol. 9, pp. E39–E47, ISBN 978-959-7136-67-5.
26 IGACC, Instituto de Geografía, Academia de Ciencias de Cuba, *Climatic Conditions. Atlas of Camagüey, Nature Section*, Academy Publishing, La Habana, (In Spanish), 1989, pp. 10–11.
27 M. V. Karyampudi, S. P. Palm, J. A. Reagen, H. Fang, W. B. Grant, R. M. Hoff, C. Moulin, H. F. Pierce, O. Torres, E. V. Browell and S. H. Melfi, Validation of the Saharan Dust Plume Conceptual Model Using Lidar, Meteosat, and ECMWF Data, *Bull. Am. Meteorol. Soc.*, 1999, **80**(6), 1045.
28 S. Mogo, V. E. Cachorro, M. Sorribas and A. M. de Frutos, Optical properties of Atmospheric PM fractions related with air masses in the central Iberian Peninsula, *Opt. Pura y Apl.*, 2006, **39**(4), 331–340.
29 E. Montilla, S. Mogo, V. E. Cachorro and A. M. de Frutos, An integrating sphere spectral system to measure continuous spectra of aerosol absorption coefficient, *J. Aerosol Sci.*, 2011, **42**, 204–212.
30 K. Fischer, Mass absorption coefficients of natural aerosol particles in the 0.4 to 2.4 μm wavelength interval, *Contrib. Atmos. Phys.*, 1973, **46**, 89.
31 J. Heintzenberg, Size-segregated measurements of particulate elemental carbon and aerosol light absorption at remote arctic locations, *Atmos. Environ.*, 1982, **16**(10), 2461–2469.
32 S. Mogo, V. E. Cachorro, M. Sorribas, A. M. de Frutos and R. Fernández, Measurements of continuous spectra of atmospheric absorption coefficients from UV to NIR *via* optical method, *Geophys. Res. Lett.*, 2005, **32**, L13811, DOI: 10.1029/2005GL022938.
33 J. R. Herman, P. K. Bhartia, O. Torres, C. Hsu, C. Seftor and E. Celarier, Global distribution of UV-absorbing aerosols from Nimbus7/TOMS data, *J. Geophys. Res.*, 1997, **201**, 16911–16922.
34 X. Querol, A. Alastuey, M. Viana, S. Rodriguez, B. Artiñano, P. Salvador, S. Garcia do Santos, R. Fernandez Patier, C. Ruiz, J. de la Rosa, A. Sanchez de la Campa, M. Menendez and J. Gil, Speciation and origin of PM10 and PM2.5 in Spain, *J. Aerosol Sci.*, 2005, **35**, 1151–1172.
35 S. Ohta and T. Okita, A chemical characterization of atmospheric aerosol in Sapporo, *Atmos. Environ., Part A*, 1990, **24**(4), 815–822.
36 B. Mason, *Principles of Geochemistry*, Wiley and Sons, New York, 1996.
37 R. Tsitouridou, D. Voutsa and Th. Kouimtzis, Ionic composition of PM10 in the area of Thessaloniki, Greece, *Chemosphere*, 2003, **52**, 883–891.
38 T. Wilson, *Salinity and the major elements of seawater*, *Chemical Oceanography*, in J. P. Riley, G. Skirrow, ed. Academic, Orlando, FL, 1995, pp. 365–413.
39 S. Mogo, V. E. Cachorro and A. M. de Frutos, Morphological, Chemical and optical absorbing characterization of aerosols in the urban atmosphere of Valladolid, *Atmos. Chem. Phys.*, 2005, **5**, 2739–2748.
40 T. C. Bond and R. Bergstrom, Light absorption by carbonaceous particles: an investigative review, *Aerosol Sci. Technol.*, 2006, **40**, 27–67.
41 D. A. Lack and C. D. Cappa, Impact of brown and clear carbon on light absorption enhancement, single scatter albedo and absorption wavelength dependence of black carbon, *Atmos. Chem. Phys.*, 2010, **10**, 4207–4220, DOI: 10.5194/acp-10-4207-2010.
42 P. Fialho, A. Hansen and R. Honrath, Absorption coefficients by aerosols in remote areas: A new approach to decouple dust and black carbon absorption coefficients using seven-wavelength aethalometer data, *J. Aerosol Sci.*, 2005, **36**, 267–282.
43 N. A. Marley, J. S. Gaffney, M. Tackett, N. C. Sturchio, L. Heraty, N. Martinez, K. D. Hardy, A. Marchany-Rivera,

T. Guilderson, A. MacMillan and K. Steelman, The impact of biogenic carbon sources on aerosol absorption in Mexico City, *Atmos. Chem. Phys.*, 2009, **9**, 1537–1549.

44 R. W. Bergstrom, K. S. Schmidt, O. Coddington, P. Pilewskie, H. Guan, J. M. Livingston, J. Redemann and P. B. Russell, Aerosol spectral absorption in the Mexico City area: results from airborne measurements during MILAGRO/INTEX B, *Atmos. Chem. Phys.*, 2010, **10**, 6333–6343, DOI: 10.5194/acp-10-6333-2010.

45 D. Encinas and H. Casado, Rain-aerosol coupling in a rural area in the Basque Country (Spain): Scavening ratios, *Aerosol Sci. Technol.*, 1999, **30**, 411–419.

46 HYSPLIT, Model. at NOAA ARL website, 2009, http://www.arl.noaa.gov/ready/.